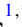






**Growth of entanglement entropy under local projective measurements**Michele Coppola <sup>1,\*</sup>, Emanuele Tirrito <sup>2,\*</sup>, Dragi Karevski <sup>1</sup> and Mario Collura <sup>2,3</sup><sup>1</sup>*Université de Lorraine, CNRS, LPCT, F-54000 Nancy, France*<sup>2</sup>*SISSA, Via Bonomea 265, 34136 Trieste, Italy*<sup>3</sup>*INFN, Via Bonomea 265, 34136 Trieste, Italy* (Received 18 October 2021; revised 10 February 2022; accepted 14 February 2022; published 9 March 2022)

Nonequilibrium dynamics of many-body quantum systems under the effect of measurement protocols is attracting an increasing amount of attention. It has been recently revealed that measurements may induce an abrupt change in the scaling law of the bipartite entanglement entropy, thus suggesting the existence of different nonequilibrium regimes. However, our understanding of how these regimes appear and whether they survive in the thermodynamic limit is much less established. Here we investigate these questions on a one-dimensional quadratic fermionic model: this allows us to reach system sizes relevant in the thermodynamic sense. We show that local projective measurements induce a qualitative modification of the time growth of the entanglement entropy which changes from linear to logarithmic. However, in the stationary regime, the logarithmic behavior of the entanglement entropy does not survive in the thermodynamic limit and, for any finite value of the measurement rate, we numerically show the existence of a single area-law phase for the entanglement entropy. Finally, exploiting the quasiparticle picture, we further support our results by analyzing the fluctuations of the stationary entanglement entropy and its scaling behavior.

DOI: [10.1103/PhysRevB.105.094303](https://doi.org/10.1103/PhysRevB.105.094303)**I. INTRODUCTION**

Recently, there has been great interest in studying the quench dynamics of isolated quantum many-body systems, where a global parameter of the Hamiltonian is suddenly changed and the initial state is left to evolve unitarily. In this scenario the quantum entanglement represents an invaluable tool to access the intrinsic nature of underlying states and their nonequilibrium properties [1–3]. In the case of unitary evolution, for local short-ranged Hamiltonians, the spreading of correlation typically scales in time, the front being bounded by a maximum propagation velocity of the information (as predicted by the Lieb-Robinson bound [4]). As a consequence, the bipartite entanglement of a semi-infinite subsystem will grow unbounded: for integrable models, where particle excitations are stable and propagate ballistically, the entanglement growth is linear in time, as predicted by the celebrated Cardy-Calabrese quasiparticle picture [5–8]. In this case, the system thermalizes (in a generalized Gibbs sense) and it is characterized by highly entangled eigenstates, i.e., states following an extensive (with the volume) scaling of their entanglement entropy [9–11].

Many factors may affect the nonequilibrium dynamics, and the scaling behavior of entanglement entropy could vary in out-of-equilibrium driving [12–15]. A paradigmatic example is that of many-body localization (MBL), in which the entanglement transition is driven by the strength of a local disordered potential [16–22]. As a result of avoiding thermalization in the MBL, the stationary state exhibits area-law

entropy for the short-entangled systems, and the entanglement entropy grows logarithmically in time, which is in contrast with linear growth in the thermalized case [22,23].

Recently, an alternative way to realize nonthermalizing states has been proposed by the use of projective measurements that influence the entanglement dramatically [24,25]. In particular, it has been established that quantum systems subjected to both measurements and unitary dynamics offer another class of dynamical behavior described in terms of quantum trajectories [26], and well explored in the context of quantum circuits [27–44], quantum spin systems [45–54], trapped atoms [55], and trapped ions [56–58]. In this context, the most celebrated phenomenon is the quantum Zeno effect [59–63] according to which continuous projective measurements can freeze the dynamics of the system completely. This question has been addressed in many-body open systems [24,64–69] whose dynamics is described by a Lindblad master equation [70–72].

In light of these developments, here we study the competition between the unitary dynamics and the random projective measurements in a noninteracting spinless fermion system. In particular, we investigate how the bipartite entanglement entropy and its fluctuations are affected by the monitoring of local degrees of freedom in a true Hamiltonian extended model.

As a main result, we find that the volume-law phase is absent for any measurement rate to subextensive entanglement content. In particular, during the initial time-dependent transient, any finite measurement rate induces an abrupt change of the entanglement, whose linear ramp suddenly changes to logarithmic growth. Moreover, we have numerical evidence that the average of the stationary entanglement entropy shows

\*These authors contributed equally to this work.

a single transition from the volume- to the area-law phase for any measurement rate in the thermodynamic limit. However, for any finite subsystem size, a remnant of a logarithmic scaling is observed, and a characteristic scaling law at a size-dependent measurement rate is established.

## II. PROTOCOL

Let us consider a quantum many-body system in one dimension, whose total Hilbert space  $\mathcal{H} = \bigotimes_j \mathcal{H}_j$ , is the tensor product of the single-particle Hilbert spaces  $\mathcal{H}_j$ . The system is originally isolated from the environment and the dynamics obeys the Schrödinger equation  $|\Psi(t)\rangle = \exp\{-it\hat{H}\}|\Psi(0)\rangle$ , where, in our protocol, the initial state is not an eigenstate of the Hamiltonian  $\hat{H}$ , and it is typically a very short-correlated state, e.g., a product state  $|\Psi(0)\rangle = \bigotimes_j |\phi_j\rangle$ .

In our protocol, the unitary dynamics is perturbed by random interactions with local measuring apparatus: namely, each single local (in real space) Hilbert space  $\mathcal{H}_j$  is coupled for a very short period of time with the environment, and a local observable  $\hat{O}_j = \sum_{k=1}^K o_k \hat{P}_j^{(k)}$  is measured. Here  $o_k$  is a possible outcome of the measurements, and  $\hat{P}_j^{(k)}$  is the projector to the corresponding subspace, with  $\sum_{k=1}^K \hat{P}_j^{(k)} = \hat{1}_j$ . Given a time step  $dt$  and a characteristic rate  $1/\tau$ , each single local degree of freedom is independently monitored; the state  $|\Psi\rangle$  is projected according to the Born rule

$$|\Psi\rangle \rightarrow \frac{\hat{P}_j^{(k)}|\Psi\rangle}{\sqrt{p_k}}, \quad (1)$$

with probability  $p_k = \langle\Psi|\hat{P}_j^{(k)}|\Psi\rangle$ .

In practice, a random number  $p \in (0, 1]$  is extracted, and a projection to the  $k$ th subspace is performed whether  $\sum_{l=1}^{k-1} p_l < p \leq \sum_{l=1}^k p_l$ . Under this dynamical protocol, the many-body state  $|\Psi(t)\rangle$  is therefore conditioned by the set of measurement events and subsequent outcomes, but it remains pure all along the protocol.

Let  $\hat{\rho}_i$  denote the density operator for the particular quantum trajectory  $\mathcal{T}_i$ ,  $\hat{\rho}_i$  being a projector. Let  $\mathcal{O}[\hat{\rho}]$  be a general functional of the density operator. In the following,  $\overline{\mathcal{O}}$  will denote the average over all the trajectories. In general,

$$\overline{\mathcal{O}^j} = \frac{1}{N} \sum_{i=1}^N (\mathcal{O}[\hat{\rho}_i])^j, \quad \forall j \geq 1 \quad (2)$$

where  $N$  is the number of quantum trajectories. Let  $\overline{\hat{\rho}} = \frac{1}{N} \sum_{i=1}^N \hat{\rho}_i$  be the average density operator:  $\overline{\mathcal{O}} = \mathcal{O}[\overline{\hat{\rho}}]$  only if  $\mathcal{O}$  is a linear functional of  $\hat{\rho}$ .

Let us mention that, although the stochastic nature of the measurement events remains, the probabilistic outcome of a quantum projective measure can be circumvented by introducing the statistical mixture; indeed, if a measurement is performed but the result of that measurement is unknown, the state is not pure anymore and transforms according to  $\hat{\rho} \rightarrow \sum_{k=1}^K \hat{P}_j^{(k)} \hat{\rho} \hat{P}_j^{(k)}$ , where at the beginning  $\hat{\rho}(0) = |\Psi(0)\rangle\langle\Psi(0)|$ . The two approaches are indistinguishable as far as we are considering observables which are linear functionals of the density operator  $\hat{\rho}(t)$ .

## A. Hopping fermions

Specifically, we apply our protocol to noninteracting spinless fermions hopping on a ring with  $L$  lattice sites. The Hamiltonian with periodic boundary conditions (PBC) reads as

$$\hat{H} = -\frac{1}{2} \sum_{j=0}^{L-1} (\hat{c}_j^\dagger \hat{c}_{j+1} + \hat{c}_{j+1}^\dagger \hat{c}_j) = \sum_{k=-L/2}^{L/2-1} \epsilon_k \hat{\eta}_k^\dagger \hat{\eta}_k, \quad (3)$$

which is diagonal in terms of the fermionic Fourier modes  $\hat{\eta}_k = \frac{1}{\sqrt{L}} \sum_{j=0}^{L-1} e^{-i2\pi k j/L} \hat{c}_j$ , with single-particle energies  $\epsilon_k = -\cos(2\pi k/L)$ . The Hamiltonian commutes with the total number of particles  $\hat{N} = \sum_j \hat{n}_j = \sum_k \hat{\eta}_k^\dagger \hat{\eta}_k$ . Due to its quadratic nature, the unitary dynamics preserves the Gaussianity of the state, i.e., Wick theorem applies. In practice, in case of closed quantum systems, whenever no measurement occurs, the two-point function  $\mathbb{C}_{ij}(t) = \langle \hat{c}_i^\dagger(t) \hat{c}_j(t) \rangle$  evolves according to  $\mathbb{C}(t+s) = \mathbb{R}^\dagger(s) \mathbb{C}(t) \mathbb{R}(s)$ , where the elements of the matrix  $\mathbb{R}(s)$  are

$$\begin{aligned} \mathbb{R}_{mn}(s) &= \frac{1}{L} \sum_{j=-L/2}^{L/2-1} e^{-i2\pi(m-n)j/L - i\epsilon_j s} \\ &\sim i^{m-n} J_{m-n}(s) \quad \text{for } L \sim \infty, \end{aligned} \quad (4)$$

$J_k(z)$  being the Bessel function of the first kind.

We focus on a dynamical protocol where we measure the local occupation number  $\hat{n}_j = \hat{c}_j^\dagger \hat{c}_j$ , which is *quadratic* in the fermions. Projective measurements could in principle destroy the Gaussian property of the state; however, we shall demonstrate that these particular measurements do not spoil such a property. By hypothesis,  $\rho \propto e^{\sum_{ij} \mathbb{M}_{ij} \hat{c}_i^\dagger \hat{c}_j}$  where  $\mathbb{M}$  is given coefficient matrix. Due to the spectral decomposition,  $\hat{n}_j = 1 \cdot \hat{P}_j^{(1)} + 0 \cdot \hat{P}_j^{(0)}$ . Moreover,  $\hat{n}_j$  is a hypermaximal Hermitian operator and, thus,  $\hat{1}_j = \hat{P}_j^{(1)} + \hat{P}_j^{(0)}$ . In this way, we have just proved that each local number operator is itself a projector ( $\hat{n}_j = \hat{P}_j^{(1)}$  and  $\hat{1}_j - \hat{n}_j = \hat{P}_j^{(0)}$ ). Second,  $\hat{P}_j^{(1)}$  and  $\hat{P}_j^{(0)}$  can be written as the limit of Gaussian operators, namely,  $\hat{n}_j = \lim_{\alpha \rightarrow \infty} e^{\alpha \hat{n}_j} / (e^\alpha - 1)$  and  $\hat{1}_j - \hat{n}_j = \lim_{\alpha \rightarrow \infty} e^{-\alpha \hat{n}_j}$ . Finally,  $e^{\pm \alpha \hat{n}_j} e^{\sum_{ij} \mathbb{M}_{ij} \hat{c}_i^\dagger \hat{c}_j} e^{\pm \alpha \hat{n}_j} = e^{\sum_{ij} \mathbb{K}_{ij}^\pm \hat{c}_i^\dagger \hat{c}_j}$  where  $\mathbb{K}^\pm$  is a new matrix whose elements are given by the Baker-Campbell-Hausdorff formula. Therefore, our protocol preserves the Gaussianity of the state.

Since occupation operators acting on different lattice sites commute, we can apply the following projecting procedure in any arbitrary order; specifically, if at time  $t$  the  $k$ th site has been measured, following the prescription in Eq. (1), if the outcome is 1 then the state projects as  $|\Psi(t)\rangle \rightarrow \hat{n}_k |\Psi(t)\rangle / \sqrt{\langle\Psi(t)|\hat{n}_k|\Psi(t)\rangle}$ , otherwise (outcome 0) the state projects  $|\Psi(t)\rangle \rightarrow (1 - \hat{n}_k) |\Psi(t)\rangle / \sqrt{\langle\Psi(t)|1 - \hat{n}_k|\Psi(t)\rangle}$ . The resulting state remaining Gaussian, we can thus focus on the two-point function  $\mathbb{C}_{ij}(t)$  which completely characterizes the entire system. The recipe is the following: for each time step  $dt$  and each chain site  $k$ , we extract a random number  $q_k \in (0, 1]$  and only if  $q_k \leq dt/\tau$  we take the measurement of the occupation number  $\hat{n}_k$ . In such case, we extract another random number  $p_k \in (0, 1]$ : if  $p_k \leq \mathbb{C}_{kk}(t) = \langle \hat{n}_k(t) \rangle$ , then thanks to the Wick theorem, the two-point function

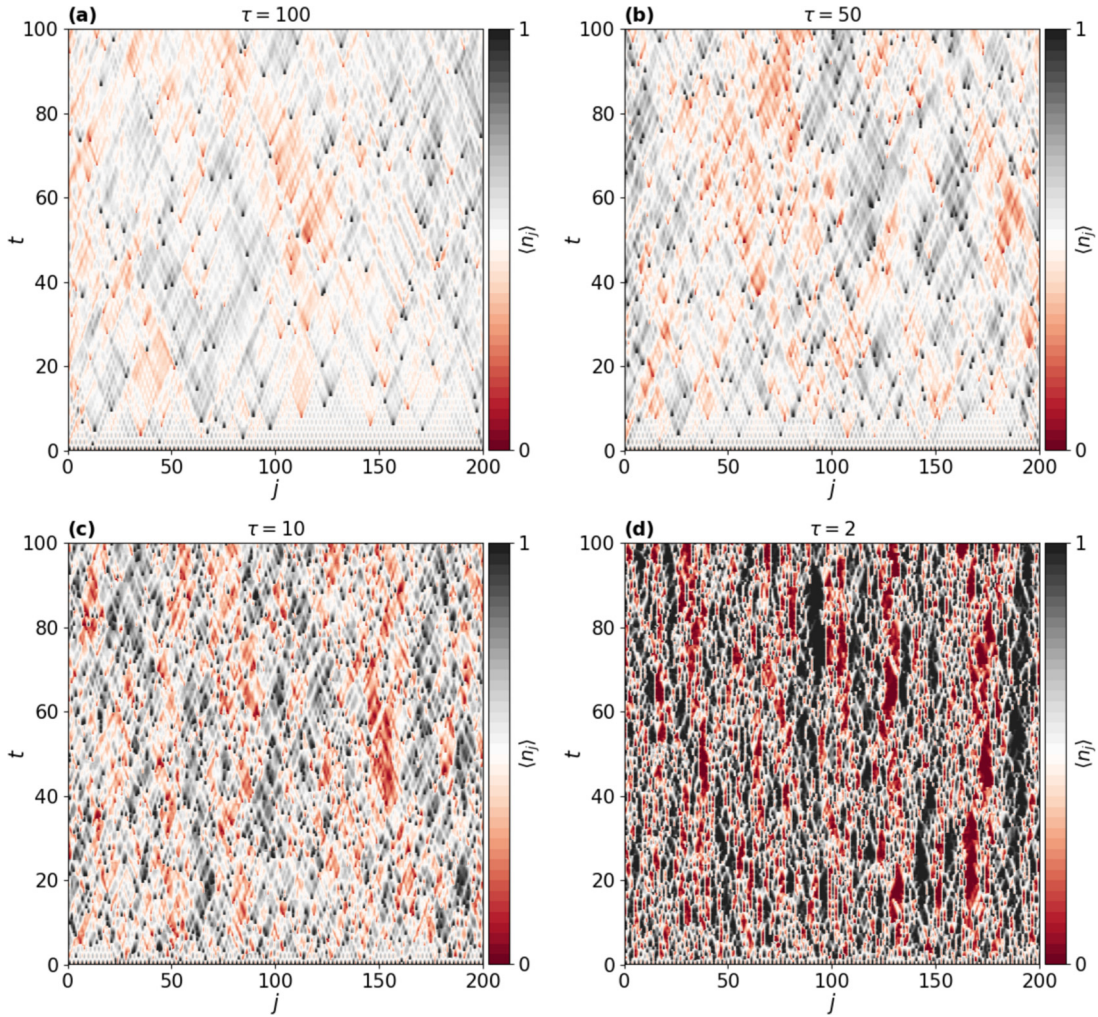


FIG. 1. Evolution of particle density: The local particle density after quenching the Néel state. The different panels represent a typical trajectory where random projective measurements of the local occupation  $\hat{n}_j$  occur with different rates  $1/\tau$ .

transforms as

$$\mathbb{C}_{ij}(t) \rightarrow \delta_{ik}\delta_{jk} + \mathbb{C}_{ij}(t) - \frac{\mathbb{C}_{ik}(t)\mathbb{C}_{kj}(t)}{\mathbb{C}_{kk}(t)}, \quad (6)$$

otherwise, if  $p_k > \mathbb{C}_{kk}(t)$ , one obtains

$$\mathbb{C}_{ij}(t) \rightarrow -\delta_{ik}\delta_{jk} + \mathbb{C}_{ij}(t) + \frac{[\delta_{ik} - \mathbb{C}_{ik}(t)][\delta_{jk} - \mathbb{C}_{kj}(t)]}{1 - \mathbb{C}_{kk}(t)}. \quad (7)$$

Let us mention that, if we lose the result of the measurements, thus introducing a statistical mixture at every measurement, this will definitely spoil the Gaussian nature of the dynamics. Therefore, we would lose the great advantage of working with a noninteracting theory. For such reason, we will always consider pure-state evolution along quantum trajectories.

In Fig. 1 we show the typical evolution of the particle density when starting from the Néel product state  $\prod_{j=0}^{L/2-1} \hat{c}_{2j}^\dagger |0\rangle$  for a system with  $L = 200$  lattice sites. Without measurements, the evolution follows the ordinary melting dynamics, and the states relax (in a local sense) toward the infinite temperature density matrix. Typically, local measurements, when very dilute in time ( $\tau \gg 1$ ), generate spikes on top

of the infinite temperature landscape, provided that correlation functions are characterized by a typical finite relaxation time. However, such local excitations, namely,  $\hat{n}_j$  or  $1 - \hat{n}_j$  with almost equal probability, propagates, and survive for “infinite” time; indeed, when a local measurement occurs in the infinite-temperature background, the local density at the measured site will relax as  $\langle \hat{n}_j(t) \rangle \simeq [1 \pm J_0(2t)]/2$ , with  $J_0(2t) \sim t^{-1/2}$ ; moreover, the connected correlation function  $\langle \hat{n}_j(t)\hat{n}_0(t) \rangle_c = \langle \hat{n}_j(t)\hat{n}_0(t) \rangle - \langle \hat{n}_j(t) \rangle \langle \hat{n}_0(t) \rangle \simeq J_j^2(2t)/4$  spreads ballistically and the front of the light cone (at  $j = 2t$ ) behaves as  $\langle \hat{n}_{2t}(t)\hat{n}_0(t) \rangle_c \sim t^{-2/3}$ . Since free quasi-particles have an infinite lifetime, they do modify the infinite-temperature landscape at arbitrary distances; as a consequence, we may expect that local projective measurements should affect the unitary dynamics even for infinitesimally small rate  $1/\tau$ , due to the power-law decay of such ballistically propagating excitations.

## B. Entanglement entropy dynamics

One quantity which is definitely affected by the random projective measurements is the bipartite entanglement entropy (EE). For a pure state  $|\Psi\rangle$ , the EE between a subsystem  $\mathcal{S}$ , and

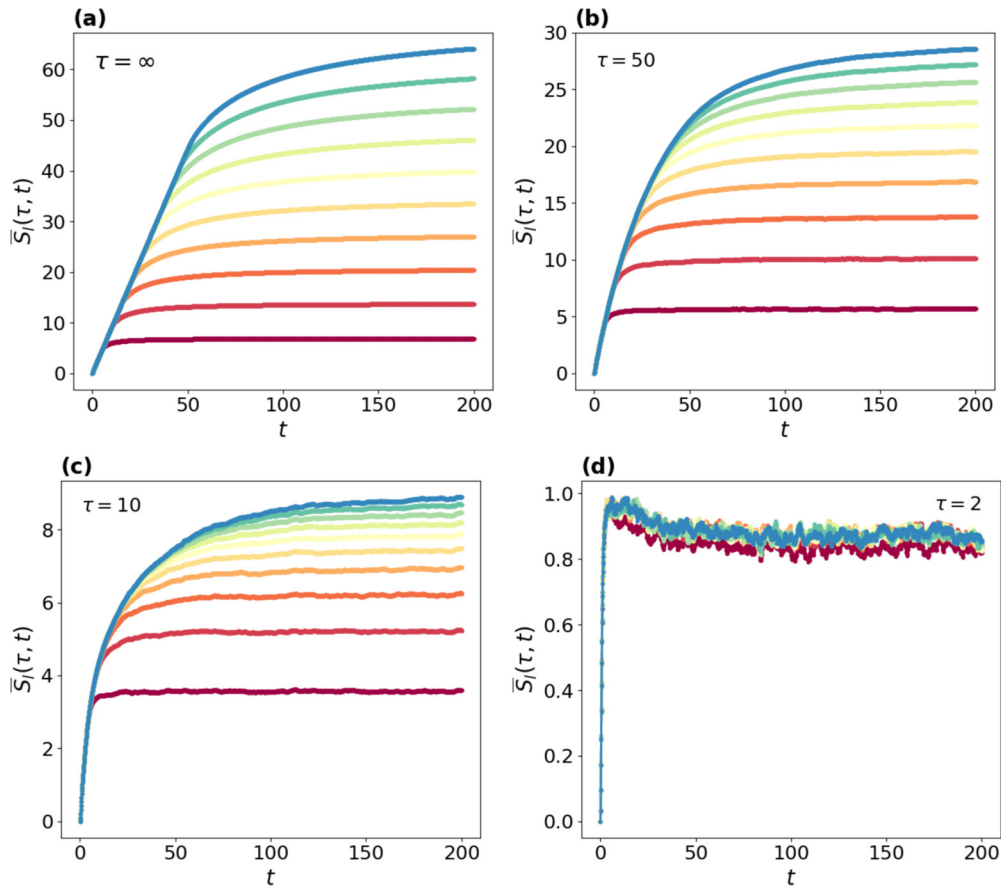


FIG. 2. Entanglement entropy vs time: EE after quenching the Néel state for a system with size  $L = 500$ . Lines, from bottom to top, represent increasing subsystem sizes  $l \in \{10n : n \in \mathbb{N} \wedge n \leq 10\}$ . The results for finite values of  $\tau \in \{2, 10, 50, \infty\}$  have been obtained by averaging over 1000 different quantum trajectories.

the rest of the system  $S^*$ , is given by  $S = -\text{Tr}_S[\hat{\rho}_S \ln \hat{\rho}_S]$ , where  $\hat{\rho}_S = \text{Tr}_{S^*}|\Psi\rangle\langle\Psi|$  is the reduced density matrix.

In the hopping fermion case, where the dynamical protocol preserves the Gaussianity of the state, the time-dependent entropy, for a subsystem consisting of  $l$  contiguous lattice sites can be evaluated as [5,73–75]

$$S_l(t) = - \sum_k \{ \lambda_k(t) \ln \lambda_k(t) + [1 - \lambda_k(t)] \ln [1 - \lambda_k(t)] \}, \quad (8)$$

where  $\lambda_k(t)$  are the eigenvalues of the subsystem two-point correlation function  $\mathbb{C}(t)|_l$ .  $\mathbb{C}(t)|_l$  is an  $l \times l$  matrix such that  $\mathbb{C}_{ij}(t)|_l = \mathbb{C}_{ij}(t) \forall i, j \in [0, l]$ .

When no measurements occur, the dynamics when starting from the Néel state is typically characterized by a *linear increase* for  $t \leq l/2$  (quasiparticle velocity  $c = 1$ ), followed by a regime where the entropy is saturating toward an *extensive* stationary value equal to  $l \ln(2)$ . In the opposite case, namely, when  $\tau \rightarrow 0$  and we keep measuring the system everywhere at every time, the state remains completely factorized and the EE is identically vanishing.

In general, a finite rate of random projective measurements should lower the entanglement production. However, it is much less clear how this in practice takes place: In particular, are both regimes affected in the same way? Is there any abrupt

change in the qualitative behavior of the entanglement, or this change smoothly depends on the measurements rate  $\tau^{-1}$ ?

We systematically study these questions by analyzing the dynamics of the bipartite EE for different subsystems of sizes  $l$ , embedded in a system of size  $L$ . We performed averages over 200–1000 different quantum trajectories depending on the specific protocol and system size. At the time  $t = 0$  the system is prepared in the Néel state.

In Fig. 2, we show the typical behavior of the bipartite EE for  $l \in \{10n : n \in \mathbb{N} \wedge n \leq 10\}$  and system size  $L = 500$ . Maximum time and subsystem sizes have been chosen in such a way that data are not affected by finite- $L$  effects.

For  $\tau = \infty$  [Fig. 2(a)], the entropy increases linearly in time and then saturates at asymptotic values which increase linearly with the subsystem size, thus manifesting the expected extensive behavior of the stationary EE in accordance with a volume law  $l \ln(2)$ . Decreasing  $\tau$ , the linear growth of the EE suddenly changes to a logarithmic growth [see Figs. 2(b) and 2(c)] in accordance to  $\bar{S}_l(t) = a_\tau \ln t + b_\tau$  which eventually saturates at large time. Finally, for very small value of  $\tau$  [see Fig. 2(d)], we have numerical evidence that the EE shows a rapid saturation to a plateau which is independent of the subsystem size. Moreover, from the bipartite EE at  $l = L/4$  we extract the parameter  $a_\tau$  by fitting the data with  $t \in [0, L/8]$ . In Fig. 3 we show  $a_\tau$  as a function of the measurement rate  $1/\tau$ , for different system sizes

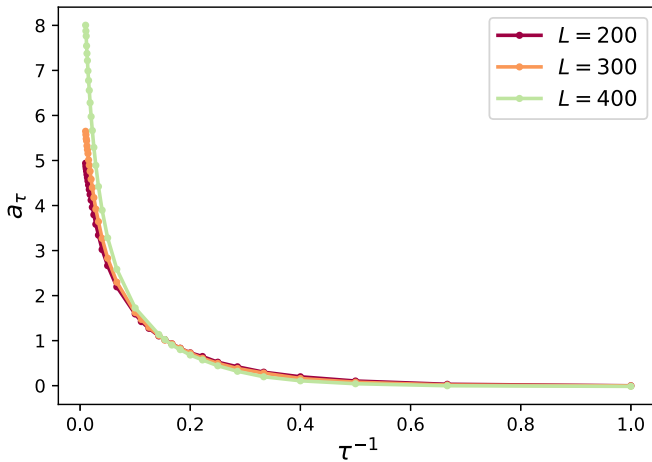


FIG. 3. Logarithmic growth: Logarithmic slope of the EE extracted from  $\bar{S}_l(t) = a_\tau \ln t + b_\tau$  at  $l = L/4$  as a function of  $\tau$  for different system sizes ( $L = 200, 300, 400$ ). It shows that when  $\tau$  is getting larger, the expected linear increase of the entanglement is restored. On the contrary, when  $\tau \rightarrow 0$ ,  $a_\tau$  is getting closer to zero, suggesting an area-law phase.

$L \in \{200, 300, 400\}$ . As expected,  $a_\tau$  is growing when  $\tau$  is getting larger, eventually diverging for  $\tau \rightarrow \infty$ , so as to restore the expected linear increase of the entanglement when no measurement occurs. On the contrary, for  $\tau \rightarrow 0$ ,  $a_\tau$  is vanishing.

Of course, the larger  $\tau$ , the larger the times and the larger the subsystems have to be in order to appreciate the deviation from the standard linear growth. Notice that, since for smaller  $\tau$  much more measures occur, in principle, one needs to take averages over a larger number of quantum trajectories in order to smooth down the random fluctuations.

Interestingly, a finite rate of projective measurements also affects the scaling of the stationary value of the EE. From a qualitative inspection of the data, the stationary value of the EE undergoes a qualitative change as well: from being extensive when  $\tau = \infty$ , it shows an area-law scaling for high rates  $1/\tau$ . However, it is less clear if the area-law behavior also applies for any finite measurement rate or not. Does another phase exist between those two asymptotic cases? In other terms, does it exist a critical measurement rate at which we observe a new *logarithmic* phase? If yes, can we determine its value? In the following, we go deep to give a definitive answer.

### C. Stationary entanglement entropy

We start our analysis of the stationary behavior of the bipartite EE as a function of the subsystem sizes and measurement rates  $1/\tau$ . Within the zero entanglement when  $\tau = 0$  and the volume-law scaling when  $\tau = \infty$ , we want to study if the stationary EE shows the intermediate logarithmic behavior when  $\tau$  is tuned and the possible existence of a finite critical parameter  $\tau_c > 0$  which may separate the logarithmic regime from the area-law regime.

To address this question, we inspect the stationary EE as a function of the subsystem size  $l$ , and different system sizes  $L$ . By convention and in order to reduce the fluctuations, we

also take the time average over the time window  $[t_{\min}, t_{\max}]$  wherein the entanglement is almost constant, where  $t_{\min} \geq l/2$  and  $t_{\max} \leq (L-l)/2$  have been chosen so that the entropy is weakly affected by finite-size effects; in fact, in that interval, the EE has essentially entered the stationary regime and is not affected by the motion of particles under PBC on a finite ring. In the following,  $\langle \cdot \rangle$  will denote the time average of any functional in that time interval.

By an analysis of the data, we conclude that the entanglement entropy saturates to a constant value independent on  $l$  for a sufficiently small value of  $\tau$ ; in other words, the measurement rate is so high that the time-evolved system cannot escape from a short correlated state. We can safely say that the system is in a Zeno-type regime in which the measurements have suppressed the entanglement, giving rise to an area-law scaling.

In order to verify if the asymptotic scaling acquires a logarithmic dependence with the subsystem size for increasing values of the parameter  $\tau$ , we make use of a linear fit  $r \ln(l) + k$  of the data with  $l \in [l_{\min}, l_{\max}]$  and we extract the parameter  $r$ : it gives an estimate of the asymptotic logarithmic slope of the entanglement, namely,  $l \partial_l \langle \bar{S}_l(\infty) \rangle$ , as a function of the measurement rates  $1/\tau$ . Here,  $l_{\min}$  and  $l_{\max}$  have been chosen depending on the system size  $L$  in order to stay in the correct regime.

In Fig. 4(b) we plot the best-fit parameter  $r$  for  $\tau \in [1, 10]$ , and different system sizes  $L \in \{200, 400, 800\}$ . This quantity is an indicator of a possible sharp transition between different regimes in the asymptotic scaling of the EE. Similarly to what has been observed for the scaling of the entropy in the time-dependent regime, the logarithmic slope  $r$  for every system size  $L$  decreases when going toward  $\tau = 0$ . In particular, for every size  $L$ , we can identify a critical value  $\tau_L^c$  such that, for  $\tau < \tau_L^c$ ,  $r$  shows a fast convergence toward zero. To estimate  $\tau_L^c$  we perform a best fit of  $r$  for every system size whose intercept with the axis  $r = 0$  gives the critical value  $\tau_L^c$  separating the area-law phase from the logarithmic regime. Indeed, if the limit  $\lim_{L \rightarrow \infty} \tau_L^c = \tau^c$  converges to a finite value, the *logarithmic phase* manifests also in the stationary regime and  $\tau_c$  captures the phase transition point between logarithmic and area-law phase. However, the data in the inset of Fig. 4(b) suggest that  $\tau_L^c$  is linearly growing with  $L$ , and therefore the only stationary-EE phase that survives in the thermodynamic limit is indeed the area-law phase.

This statement is strongly supported by the study of the EE as a function of  $\tau$  for different subsystem sizes as shown in Fig. 5. For very high measurement rates  $1/\tau$ , the stationary EE is independent on the subsystem size  $l$  with a very good approximation. As  $\tau$  increases, the stationary EE becomes  $l$  dependent and changes its concavity at  $\tau = \tau_l^*$ . In particular, our data show a logarithmic growth of the inflection point  $\tau_l^*$  with the subsystem size  $l$ . This observation allows us to introduce a correlation length  $\xi(\tau)$  which increases exponentially with  $\tau$  and affects very much the behavior of the stationary EE. In fact, if  $\xi(\tau) \ll l$ , then only the chain's sites close to the boundary of the subsystem are correlated with the rest of the quantum system. For this reason, the EE is  $l$  independent. As  $\xi(\tau)$  gets larger and larger, more and more sites are involved in generating correlation with the rest of the chain. When  $l \sim \xi(\tau)$  the EE shows a logarithmic scaling

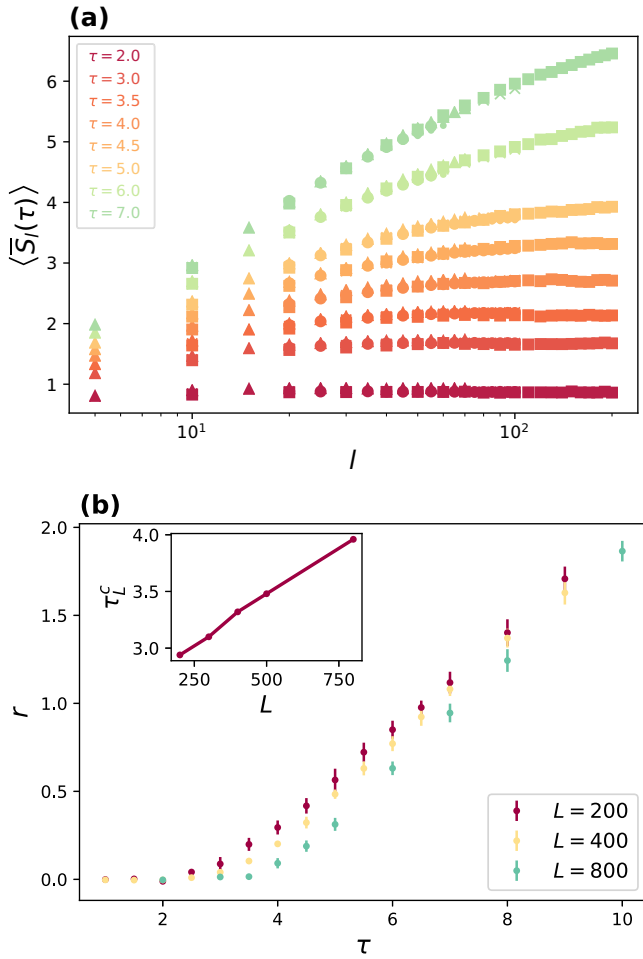


FIG. 4. The stationary entanglement: (a) Stationary EE for  $L \in \{200, 300, 400, 500, 800\}$  (different symbols) and different measurement rates  $1/\tau$  (different colors), as a function of the subsystem size  $l \in [1, 200]$ , is plotted in log-linear scale. (b) Logarithmic slope of the stationary EE extracted from different system sizes  $L$  as a function of the measurement rates  $\tau$ . The inset shows a finite-size scaling of the critical value  $\tau_l^c$  revealing its divergence increasing the system size  $L$ ; see main text for details.

with the subsystem size; however, this region moves in the parameter space  $\tau - l$  such that it eventually tends to infinity in the thermodynamic limit, thus disappearing. Finally, for  $\xi(\tau) \gg l$  the entire subsystem contributes to the EE and this essentially results in a volume-law behavior.

#### D. Entanglement entropy scaling

As well known, the generalized hydrodynamic (GHD) [76–80] makes use of a quasiparticle picture [6–8] to explain qualitatively the behavior of the entanglement dynamics. Let  $x_1$  and  $x_2$  be two general points of the chain: they define the subsystem  $\mathcal{I} = [x_1, x_2]$  of interest for the EE ( $|x_1 - x_2| = l < L$ ). For weakly entangled and excited quantum states, the EE under unitary time evolution is [24]

$$S_l(t) = \int_{-\pi}^{\pi} \frac{dk}{2\pi} \int_{\mathcal{Q}_{k,t}} dx s(x - v(k)t, k, 0), \quad (9)$$

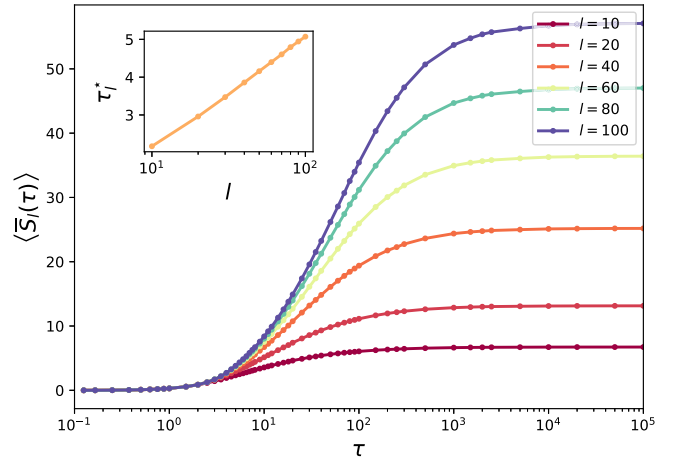


FIG. 5. Stationary entanglement entropy vs  $\tau$ : The stationary EE as a function of  $\tau$  for different subsystem sizes  $l$  and  $L = 400$ . The entropy is approximately independent on  $l$  for small values of the parameter  $\tau$ . The inset shows the divergence of the inflection point  $\tau_l^c$  for  $L = 400$  as a function of the subsystem size  $l$ .

where  $v(k) = \sin(k)$  is the group velocity of the quasiparticles,  $s(x, k, t)$  represents the contribution to the EE for a pair of quasiparticles at positions  $x$  and  $x - 2v(k)t$ , and  $\mathcal{Q}_{k,t} = \{x \in \mathcal{I} \mid x - 2v(k)t \notin \mathcal{I}\}$ .

It is interesting to notice that, in the continuous limit ( $dt \rightarrow 0$ ), the time evolution of the average density operator is given by the Lindblad equation (where the jump operators coincide with the local number operators) of which the stochastic Schrödinger equation (SSE) is an unraveling. In other terms,

$$\frac{d\bar{\rho}^{\text{CL}}}{dt} = -i[\hat{H}, \bar{\rho}^{\text{CL}}] - \frac{1}{\tau} \sum_{j=1}^L [\hat{n}_j, [\hat{n}_j, \bar{\rho}^{\text{CL}}]], \quad (10)$$

where  $\bar{\rho}^{\text{CL}}$  is the average density operator in the continuous limit (CL).

In the CL, we can use the quasiparticle picture and the postulates for the entanglement growth in presence of continuous measurements, where  $1/\tau$  represents the monitoring rate of each quasiparticle.<sup>1</sup> As put forward in Ref. [24], the idea is based on the possibility that the ballistic motion may be stopped by a random measure event which destroys a pair of quasiparticles and generates a new excitation which starts spreading from the position of one of the two old partners with the same probability  $\frac{1}{2}$ . The new quasiparticles travel with random momenta  $\pm k$  where  $|k|$  is chosen uniformly in  $[0, \pi]$ . Let  $\bar{S}_l^{\text{CL}}(\tau, t)$  denote the average EE in the CL. Using the prescriptions in [24] with the physical measurement rate  $1/\tau$ , we get

$$\bar{S}_l^{\text{CL}}(\tau, t \rightarrow \infty) = \ln(2) \int_0^\infty \frac{dy}{\tau} e^{-y/\tau} \int_{-\pi}^{\pi} \frac{dk}{2\pi} \int_{\mathcal{Q}_{k,y}} dx, \quad (11)$$

<sup>1</sup>Note that the rate used in [24] is two times bigger than the rate we deduce from (10).

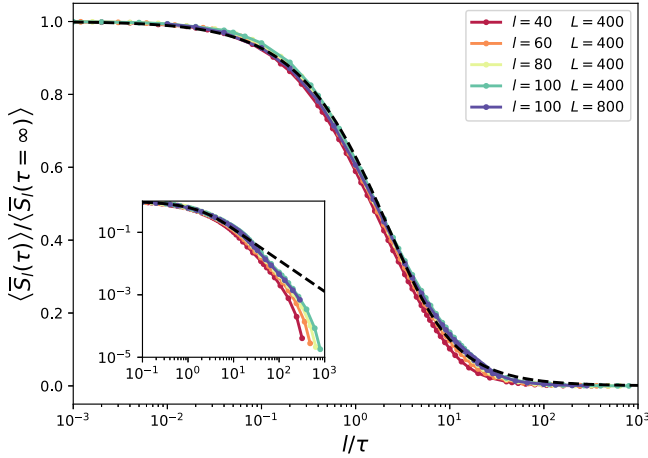


FIG. 6. Scaling of the stationary entanglement entropy: Scaling of the stationary EE:  $\lambda = l/\tau$  on the  $x$  axis;  $\langle \bar{S}_l(\tau) \rangle / \langle \bar{S}_l(\tau = \infty) \rangle$  on the  $y$  axis. The dashed line is the function  $f(\lambda)$  given by the GHD. Note that  $\langle \bar{S}_l(\tau) \rangle$  has been computed by taking the average in  $[t_{\min}, t_{\max}]$ : it means that  $\langle \bar{S}_l(\tau = \infty) \rangle$  is very well approximated by  $l \ln(2)$  only if  $l \ll L$ . The inset shows the same data in log-log scale to emphasize the differences between the models for high rates.

whose asymptotic behavior reads as

$$\frac{\bar{S}_l^{\text{CL}}(\tau, t \rightarrow \infty)}{S_l(\tau = \infty)} = f(\lambda), \quad f(\lambda) \sim \begin{cases} 1, & \lambda \ll 1 \\ \lambda^{-1}, & \lambda \gg 1 \end{cases} \quad (12)$$

where  $\lambda = l/\tau$ , and  $S_l(\tau = \infty) = \ln(2)l$  is the asymptotic value of the EE under free time evolution. Since our protocol differs from the one in Ref. [24], it is worth investigating whether our recipe agrees with their scaling result. Actually, assuming  $dt \ll 1$ , the EE in our discrete model is very well captured by the CL description when  $dt/\tau \ll 1$ . Even if we expect to have a good prediction by the GHD only for  $\tau \gg 1$ , we see in Fig. 6 that the agreement is excellent in a much wider range of measurement rates. Figure 6 also shows the same ratio for different chain sizes  $L \in \{400, 800\}$  to emphasize that it is weakly affected by finite-size effects. However, using bigger chains ensures better agreement between data and theoretical predictions, as expected.

### E. Stationary entanglement entropy fluctuations

In order to further support the results of the previous sections, we decided to analyze the EE fluctuations  $\langle \sigma_l^2(\tau) \rangle = \langle \bar{S}_l^2(\tau) \rangle - \langle \bar{S}_l(\tau) \rangle^2$ . From the numerical results, we see the following: (i) the variance is  $l$  independent for very high measurement rates; (ii) it approximately decays as  $\sim 1/\tau$  for very low rates (see Fig. 7). The behavior at low  $\tau$  is not surprising: for very high rates, we are close to the Zeno regime and then we do expect that also higher momenta of the EE are size independent. The behavior at high values of  $\tau$  may be easily understood if we look at the properties of the Poisson distribution, as detailed below. Indeed, suppose  $\tau$  is large enough in order to satisfy  $Ldt/\tau \ll 1$ ; in this case, the probability to have multiple measurement events after each time step  $dt$  is approximately zero. Under this assumption, the measurement

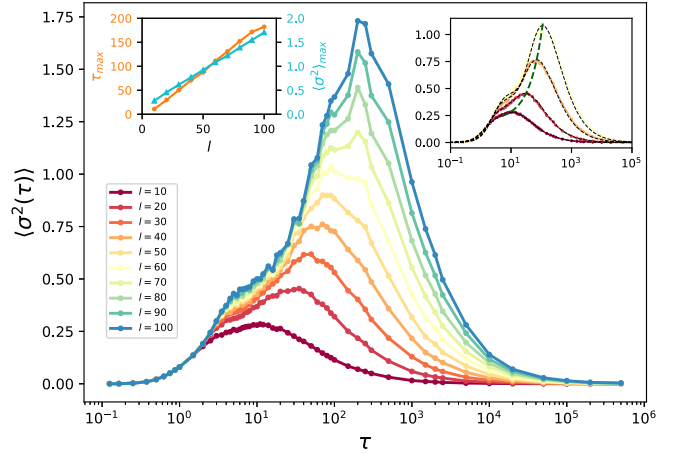


FIG. 7. Fluctuations of the stationary entanglement entropy: Fluctuations of the stationary EE as a function of the parameter  $\tau$  for  $L = 400$ . The absolute maximum point  $\langle \sigma_l^2 \rangle_{\text{max}}$  and its position  $\tau_{\text{max}}$  increase linearly with the subsystem size  $l$ , as shown in the inset on the left. The inset on the right shows some fit functions (dashed lines) with their data; the green curve interpolates their maximum points.

process becomes a Poisson process and  $\kappa = TL/\tau$  is the average number of measurements in the time interval  $[0, T]$ . It follows that

$$\bar{S}^n_l(\tau, T) = \sum_j \mathcal{P}(j) \mathcal{A}_l(j, n, T), \quad (13)$$

where  $\mathcal{P}(j) = \kappa^j e^{-\kappa} / j!$  is the probability to take  $j$  measurements in  $[0, T]$  and  $\mathcal{A}_l(j, n, T)$  is the weighted average of the  $n$ th momentum over all the quantum trajectories which can be generated in  $[0, T]$  with fixed number of measurements  $j$ . The variance is thus given by

$$\begin{aligned} \sigma_l^2(\tau, T) &= \bar{S}_l^2(\tau, T) - (\bar{S}_l(\tau, T))^2 \\ &\sim \mathcal{F}_l(T) \kappa(\tau, T), \quad \kappa \ll 1 \end{aligned} \quad (14)$$

where  $\mathcal{F}_l(T) = \mathcal{A}_l(1, 2, T) - 2\mathcal{A}_l(0, 1, T)\mathcal{A}_l(1, 1, T) + \mathcal{A}_l(0, 1, T)^2$ . Of course, we are interested in computing the stationary variance and thus  $T$  has to be large enough. It is interesting to notice that, in this regime,  $\sigma_l^2(\tau, hT) = \sigma_l^2(\tau, T)$  with  $h > 1$ . In fact, we can show that  $\mathcal{F}_l(hT) = \mathcal{F}_l(T)/h$  and  $\kappa(\tau, hT) = h\kappa(\tau, T)$ .

The term  $\mathcal{A}_l(1, n, T)$  represents the contribution for one single measurement and then it is not surprising that it can be written in terms of small perturbations with respect to the 0-measurement case. In other terms,  $\mathcal{F}_l(T)$  is approximately proportional to  $l^2$  and thus the ratio  $g(l, \tau) = \langle \sigma_l^2(\tau) \rangle / \langle \bar{S}_l(\tau) \rangle^2$  is essentially  $l$  independent and proportional to  $1/\tau$  for very low measurement rates. This behavior is emphasized in Fig. 8.

In addition to the interesting asymptotic behaviors, the variance shows a double-peak structure (see Fig. 7) which might be evidence of the existence of two different processes generating fluctuations. Note that this double-peak structure also affects the ratio  $g(l, \tau) = \langle \sigma_l^2(\tau) \rangle / \langle \bar{S}_l(\tau) \rangle^2$ , as shown in Fig. 8.

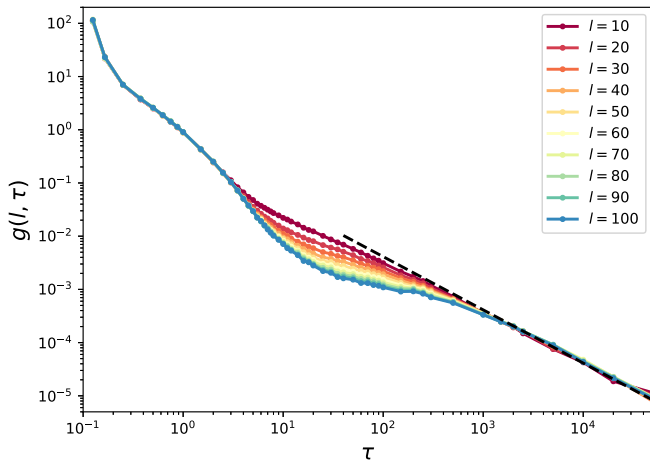


FIG. 8. Scaling of the fluctuations for small measurement rates: The ratio  $g(l, \tau) = \langle \sigma_l^2(\tau) \rangle / \langle \bar{S}_l(\tau) \rangle^2$  as a function of the parameter  $\tau$  for  $L = 400$ . The dashed line represents the asymptotic behavior obtained by theoretical argues; see main text for details.

Our data suggest that the position of the peak on the left scales logarithmically with the subsystem size  $l$ : this is not surprising because, in that regime, fluctuations reflect the behavior of the inflection point  $\tau_l^*$  of the EE which also scales logarithmically. Despite the fact that the number of simulated trajectories is not sufficient to proceed with a thorough analysis, it seems that the peak's position of the absolute maximum  $\tau_{\max}$  and its value  $\langle \sigma^2 \rangle_{\max} = \langle \sigma^2(\tau_{\max}) \rangle$  increase linearly with the subsystem size  $l$ , as shown in the inset of Fig. 7. In order to estimate the maximum points and their positions, we fit the

data with a linear combination of two functions obtained by the square of the relation (11) and the square of the average contribution to the EE of the new pairs of particles randomly created by measurements [which appears in the argument of the integral (11)]. By optimizing the parameters of these fit functions, we obtain a very good interpolation of the data, as shown in the inset of Fig. 7. This might suggest that it is possible to describe the processes generating fluctuations making use of the quasiparticle picture.

### III. DISCUSSION AND CONCLUSION

In this work, we investigated the quantum quench dynamics in a free-fermion chain under projective measurements of occupation numbers. By computing the EE of the system during the time evolution, we found that the entanglement shows a logarithmic growth in time before reaching the stationary value. Furthermore, thanks to the experimental progress, this logarithmic regime that emerges for finite-size systems can be also addressed in the laboratory [81–84].

Moreover, we also investigated the properties of the stationary EE as a function of the measurement rate  $1/\tau$  and we studied a volume- to area-law transition that emerges for any value of  $\tau$ . Finally, we studied the scaling of the stationary EE, the fluctuations, and the ratio between the variance and the square of the stationary EE as a function of the measurement rate, finding out a linear asymptotic behavior. We found a very intriguing phenomenon where the EE fluctuations are generated by two distinct processes which are both qualitatively captured by the quasiparticle picture.

- 
- [1] L. Amico, R. Fazio, A. Osterloh, and V. Vedral, *Rev. Mod. Phys.* **80**, 517 (2008).
  - [2] J. Eisert, M. Cramer, and M. B. Plenio, *Rev. Mod. Phys.* **82**, 277 (2010).
  - [3] N. Laflorencie, *Phys. Rep.* **646**, 1 (2016).
  - [4] E. H. Lieb and D. W. Robinson, *Statistical Mechanics* (Springer, Berlin, 1972), pp. 425–431.
  - [5] P. Calabrese and J. Cardy, *J. Stat. Mech.: Theory Exp.* (2005) P04010.
  - [6] V. Alba and P. Calabrese, *Proc. Natl. Acad. Sci. USA* **114**, 7947 (2017).
  - [7] V. Alba, *Phys. Rev. B* **97**, 245135 (2018).
  - [8] V. Alba and P. Calabrese, *SciPost Phys.* **4**, 017 (2018).
  - [9] M. Rigol, V. Dunjko, and M. Olshanii, *Nature (London)* **452**, 854 (2008).
  - [10] R. Nandkishore and D. A. Huse, *Annu. Rev. Condens. Matter Phys.* **6**, 15 (2015).
  - [11] D. A. Abanin, E. Altman, I. Bloch, and M. Serbyn, *Rev. Mod. Phys.* **91**, 021001 (2019).
  - [12] P. Calabrese and J. Cardy, *J. Stat. Mech.: Theory Exp.* (2007) P06008.
  - [13] C. W. von Keyserling, T. Rakovszky, F. Pollmann, and S. L. Sondhi, *Phys. Rev. X* **8**, 021013 (2018).
  - [14] T. Rakovszky, F. Pollmann, and C. W. von Keyserling, *Phys. Rev. Lett.* **122**, 250602 (2019).
  - [15] V. Alba and P. Calabrese, *Phys. Rev. B* **100**, 115150 (2019).
  - [16] D. Basko, I. Aleiner, and B. Altshuler, *Probl. Condens. Matter Phys.*, 50 (2006).
  - [17] M. Žnidarič, T. Prosen, and P. Prelovšek, *Phys. Rev. B* **77**, 064426 (2008).
  - [18] J. H. Bardarson, F. Pollmann, and J. E. Moore, *Phys. Rev. Lett.* **109**, 017202 (2012).
  - [19] S. Iyer, V. Oganesyan, G. Refael, and D. A. Huse, *Phys. Rev. B* **87**, 134202 (2013).
  - [20] H. Kim and D. A. Huse, *Phys. Rev. Lett.* **111**, 127205 (2013).
  - [21] D. A. Huse, R. Nandkishore, and V. Oganesyan, *Phys. Rev. B* **90**, 174202 (2014).
  - [22] B. Bauer and C. Nayak, *J. Stat. Mech.: Theory Exp.* (2013) P09005.
  - [23] J. A. Kjäll, J. H. Bardarson, and F. Pollmann, *Phys. Rev. Lett.* **113**, 107204 (2014).
  - [24] X. Cao, A. Tilloy, and A. De Luca, *SciPost Phys.* **7**, 024 (2019).
  - [25] B. Skinner, J. Ruhman, and A. Nahum, *Phys. Rev. X* **9**, 031009 (2019).
  - [26] H. Wiseman, *Quantum Semiclassical Opt.: J. Eur. Opt. Soc. Part B* **8**, 205 (1996).
  - [27] Y. Li, X. Chen, and M. P. A. Fisher, *Phys. Rev. B* **98**, 205136 (2018).
  - [28] Y. Li, X. Chen, and M. P. A. Fisher, *Phys. Rev. B* **100**, 134306 (2019).



- [29] Y. Li, X. Chen, A. W. Ludwig, and M. Fisher, *Phys. Rev. B* **104**, 104305 (2021).
- [30] M. Szyniszewski, A. Romito, and H. Schomerus, *Phys. Rev. Lett.* **125**, 210602 (2020).
- [31] L. Zhang, J. A. Reyes, S. Kourtis, C. Chamon, E. R. Mucciolo, and A. E. Ruckenstein, *Phys. Rev. B* **101**, 235104 (2020).
- [32] A. Zabalo, M. J. Gullans, J. H. Wilson, S. Gopalakrishnan, D. A. Huse, and J. H. Pixley, *Phys. Rev. B* **101**, 060301(R) (2020).
- [33] O. Shtanko, Y. A. Kharkov, L. P. García-Pintos, and A. V. Gorshkov, [arXiv:2004.06736](https://arxiv.org/abs/2004.06736).
- [34] C.-M. Jian, B. Bauer, A. Keselman, and A. W. Ludwig, [arXiv:2012.04666](https://arxiv.org/abs/2012.04666).
- [35] A. Nahum, J. Ruhman, S. Vijay, and J. Haah, *Phys. Rev. X* **7**, 031016 (2017).
- [36] A. Chan, R. M. Nandkishore, M. Pretko, and G. Smith, *Phys. Rev. B* **99**, 224307 (2019).
- [37] M. Szyniszewski, A. Romito, and H. Schomerus, *Phys. Rev. B* **100**, 064204 (2019).
- [38] A. Lavasani, Y. Alavirad, and M. Barkeshli, *Phys. Rev. Lett.* **127**, 235701 (2021).
- [39] A. Lavasani, Y. Alavirad, and M. Barkeshli, *Nat. Phys.* **17**, 342 (2021).
- [40] M. Block, Y. Bao, S. Choi, E. Altman, and N. Yao, *Phys. Rev. Lett.* **128**, 010604 (2022).
- [41] S. Sang and T. H. Hsieh, *Phys. Rev. Research* **3**, 023200 (2021).
- [42] B. Shi, X. Dai, and Y.-M. Lu, [arXiv:2012.00040](https://arxiv.org/abs/2012.00040).
- [43] O. Lunt and A. Pal, *Phys. Rev. Research* **2**, 043072 (2020).
- [44] P. Sierant and X. Turkeshi, [arXiv:2109.06882](https://arxiv.org/abs/2109.06882).
- [45] S. Dhar and S. Dasgupta, *Phys. Rev. A* **93**, 050103(R) (2016).
- [46] X. Turkeshi, R. Fazio, and M. Dalmonte, *Phys. Rev. B* **102**, 014315 (2020).
- [47] N. Lang and H. P. Büchler, *Phys. Rev. B* **102**, 094204 (2020).
- [48] D. Rossini and E. Vicari, *Phys. Rev. B* **102**, 035119 (2020).
- [49] X. Turkeshi, A. Biella, R. Fazio, M. Dalmonte, and M. Schiró, *Phys. Rev. B* **103**, 224210 (2021).
- [50] T. Botzung, S. Diehl, and M. Müller, *Phys. Rev. B* **104**, 184422 (2021).
- [51] T. Boorman, M. Szyniszewski, H. Schomerus, and A. Romito, [arXiv:2107.11354](https://arxiv.org/abs/2107.11354).
- [52] Y. Fuji and Y. Ashida, *Phys. Rev. B* **102**, 054302 (2020).
- [53] M. Ippoliti and V. Khemani, *Phys. Rev. Lett.* **126**, 060501 (2021).
- [54] X. Turkeshi, [arXiv:2101.06245](https://arxiv.org/abs/2101.06245).
- [55] T. J. Elliott, W. Kozłowski, S. F. Caballero-Benitez, and I. B. Mekhov, *Phys. Rev. Lett.* **114**, 113604 (2015).
- [56] S. Czischek, G. Torlai, S. Ray, R. Islam, and R. G. Melko, *Phys. Rev. A* **104**, 062405 (2021).
- [57] C. Noel, P. Niroula, A. Risinger, L. Egan, D. Biswas, M. Cetina, A. V. Gorshkov, M. Gullans, D. A. Huse, and C. Monroe, [arXiv:2106.05881](https://arxiv.org/abs/2106.05881).
- [58] P. Sierant, G. Chiriaco, F. M. Surace, S. Sharma, X. Turkeshi, M. Dalmonte, R. Fazio, and G. Pagano, *Quantum* **6**, 638 (2022).
- [59] A. Degasperis, L. Fonda, and G. Ghirardi, *Il Nuovo Cimento A (1965-1970)* **21**, 471 (1974).
- [60] B. Misra and E. G. Sudarshan, *J. Math. Phys.* **18**, 756 (1977).
- [61] A. Peres, *Am. J. Phys.* **48**, 931 (1980).
- [62] K. Snizhko, P. Kumar, and A. Romito, *Phys. Rev. Research* **2**, 033512 (2020).
- [63] A. Biella and M. Schiró, *Quantum* **5**, 528 (2021).
- [64] O. Alberton, M. Buchhold, and S. Diehl, *Phys. Rev. Lett.* **126**, 170602 (2021).
- [65] T. Müller, S. Diehl, and M. Buchhold, *Phys. Rev. Lett.* **128**, 010605 (2022).
- [66] S. Goto and I. Danshita, *Phys. Rev. A* **102**, 033316 (2020).
- [67] M. Buchhold, Y. Minoguchi, A. Altland, and S. Diehl, *Phys. Rev. X* **11**, 041004 (2021).
- [68] T. Minato, K. Sugimoto, T. Kuwahara, and K. Saito, *Phys. Rev. Lett.* **128**, 010603 (2022).
- [69] T. Maimbourg, D. M. Basko, M. Holzmann, and A. Rosso, *Phys. Rev. Lett.* **126**, 120603 (2021).
- [70] F. Carollo, R. L. Jack, and J. P. Garrahan, *Phys. Rev. Lett.* **122**, 130605 (2019).
- [71] M. Žnidarič, *Phys. Rev. E* **89**, 042140 (2014).
- [72] F. Carollo, J. P. Garrahan, I. Lesanovsky, and C. Pérez-Espigares, *Phys. Rev. E* **96**, 052118 (2017).
- [73] G. Vidal, J. I. Latorre, E. Rico, and A. Kitaev, *Phys. Rev. Lett.* **90**, 227902 (2003).
- [74] M. Fagotti and P. Calabrese, *Phys. Rev. A* **78**, 010306(R) (2008).
- [75] V. Alba, M. Fagotti, and P. Calabrese, *J. Stat. Mech.: Theory Exp.* (2009) P10020.
- [76] B. Bertini, M. Collura, J. De Nardis, and M. Fagotti, *Phys. Rev. Lett.* **117**, 207201 (2016).
- [77] O. A. Castro-Alvaredo, B. Doyon, and T. Yoshimura, *Phys. Rev. X* **6**, 041065 (2016).
- [78] V. B. Bulchandani, R. Vasseur, C. Karrasch, and J. E. Moore, *Phys. Rev. Lett.* **119**, 220604 (2017).
- [79] B. Doyon, *SciPost Phys. Lect. Notes* **18** (2020).
- [80] V. Alba, B. Bertini, M. Fagotti, L. Piroli, and P. Ruggiero, *J. Stat. Mech.: Theory Exp.* (2021) 114004.
- [81] I. Bloch, J. Dalibard, and W. Zwerger, *Rev. Mod. Phys.* **80**, 885 (2008).
- [82] R. Islam, R. Ma, P. M. Preiss, M. E. Tai, A. Lukin, M. Rispoli, and M. Greiner, *Nature (London)* **528**, 77 (2015).
- [83] A. Elben, R. Kueng, H.-Y. R. Huang, R. van Bijnen, C. Kokail, M. Dalmonte, P. Calabrese, B. Kraus, J. Preskill, P. Zoller, and B. Vermersch, *Phys. Rev. Lett.* **125**, 200501 (2020).
- [84] T. Brydges, A. Elben, P. Jurcevic, B. Vermersch, C. Maier, B. P. Lanyon, P. Zoller, R. Blatt, and C. F. Roos, *Science* **364**, 260 (2019).